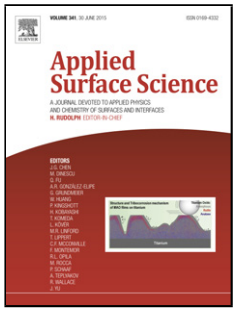


Title: Fabrication of TiO2-modified Polytetrafluoroethylene Ultrafiltration Membranes via Plasma-enhanced Surface Graft Pretreatment

Author: Yingjia Qian Lina Chi Weili Zhou Zhenjiang Yu Zhongzhi Zhang Zhenjia Zhang Zheng Jiang

PII: S0169-4332(15)02754-3
DOI: http://dx.doi.org/doi:10.1016/j.apsusc.2015.11.059
Reference: APSUSC 31776

To appear in: *APSUSC*

Received date: 13-8-2015
Revised date: 15-10-2015
Accepted date: 6-11-2015

Please cite this article as: Y. Qian, L. Chi, W. Zhou, Z. Yu, Z. Zhang, Z. Zhang, Z. Jiang, Fabrication of TiO2-modified Polytetrafluoroethylene Ultrafiltration Membranes via Plasma-enhanced Surface Graft Pretreatment, *Applied Surface Science* (2015), http://dx.doi.org/10.1016/j.apsusc.2015.11.059

Highlights

Multifunctional $TiO_2$/PAA/PTFE ultrafiltration membrane was fabricated via tight coating of $TiO_2$ functional layer onto the plasma-assisted graft of PAA on PTFE.

The high water flux rate, remarkable enhanced ultrafiltration performance and excellent self-cleaning ability were demonstrated

The formation of COO-Ti bidentate coordination between $TiO_2$ and PAA was responsible for the successful coating.

## Graphical Abstract

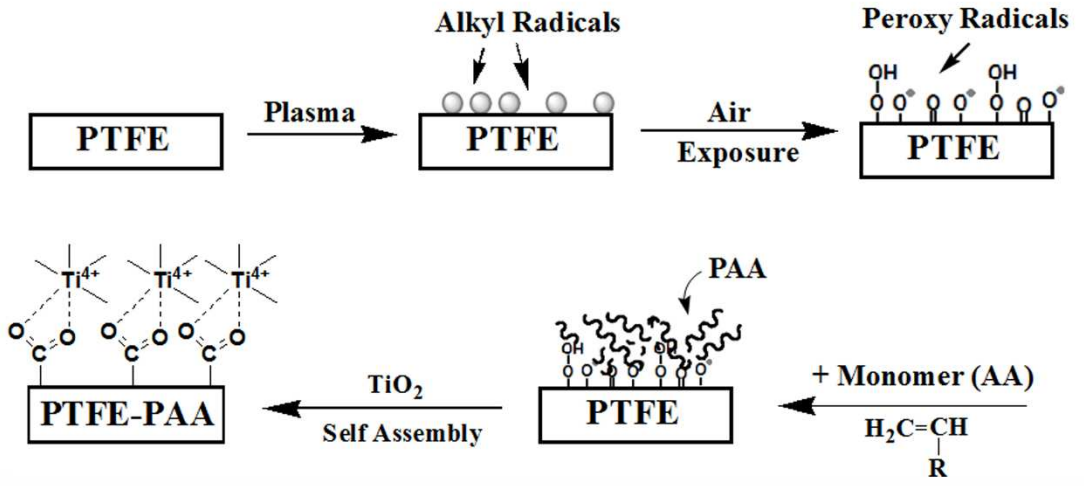

# Fabrication of $TiO_2$-modified Polytetrafluoroethylene Ultrafiltration Membranes via Plasma-enhanced Surface Graft Pretreatment

Yingjia Qian[a], Lina Chi[a,b]*, Weili Zhou[a], Zhenjiang Yu[a], Zhongzhi Zhang[c], Zhenjia Zhang[a], Zheng Jiang[b]*

a School of Environmental Science and Engineering, Shanghai Jiaotong University, Shanghai 200240, China

b Faculty of Engineering and the Environment, University of Southampton, Southampton, SO17 1BJ, UK

c College of Chemical Engineering, China University of Petroleum, Beijing 102249, China

Corresponding author. Tel.: +86 021-54747412; fax: +86 021-54740836

E-mail addresses: lnchi@sjtu.edu.cn

## ABSTRACT

Surface hydrophilic modification of polymer ultrafiltration membrane using metal oxide represents an effective yet highly challenging solution to improve water flux and antifouling performance. Via plasma-enhanced graft of poly acryl acid (PAA) prior to coating $TiO_2$, we successfully fixed $TiO_2$ functional thin layer on super hydrophobic Polytetrafluoroethylene (PTFE) ultrafiltration (UF) membranes. The characterization results evidenced $TiO_2$ attached on the PTFE-based UF membranes through the chelating bidentate coordination between surface-grafted carboxyl group and $Ti^{4+}$. The $TiO_2$ surface modification may greatly reduce the water contact angle from 115.8° of the PTFE membrane to 35.0° without degradation in 30-day continuous filtration operations. The novel $TiO_2$/PAA/PTFE membranes also exhibited excellent antifouling and self-cleaning performance due to the intrinsic hydrophilicity and photocatalysis properties of $TiO_2$, which was further confirmed by the photo-degradation of MB under Xe lamp irradiation.

Keywords:

Ultrafiltration, Polytetrafluoroethylene Membrane, Titanium dioxide ($TiO_2$), Plasma-induced Graft Polymerization

## 1. Introduction

Polytetrafluoroethylene (PTFE) possesses superior properties to many other polymers in chemical stability, thermal resistance, low water absorption, potential biocompatibility, good mechanical strength and erosion resistance, making it an attractive material for anti-corrosion coatings, fuel cell composite membranes, microelectronic packaging, biomedicine and space applications [1,2]. PTFE can

be well processed to porous fibers or thin films through solvent-free melt spinning or extrusion and post-stretching strategies. Porous PTFE membrane has also found peculiar importance in water treatment [3], separators of lithium-ion batteries [4], pervaporation [5], blood purification [6]. However, the super hydrophobicity of PTFE brings about a series of serious issues in practice. For instance, as a separation membrane in the membrane bioreactor (MBR) for wastewater purification, PTFE membranes exhibit low water flux and face low energy efficiency due to serious fouling.

Surface hydrophilic modification presents a viable solution to apply PTFE in industrial water treatment, whereas the hydrophilicity modification of PTFE faces great challenges due to its intrinsic non-polar linear molecular configuration of C and F atoms [7-9]. The main principle of surface hydrophilicity modification is to tightly coat the original hydrophobic PTFE with thin layer of hydrophilic materials[8,10-13]. As an environmentally friendly and chemically stable material, $TiO_2$ has often been applied to produce hydrophilic and antifouling composite membranes. The coated $TiO_2$ nanoparticles may also offer the composite membranes with desired self-cleaning capability since it can photocatalitically degrade organic pollutants and kill bacteria under UV light [14]. So far, to fabricate composite membranes, two major methodologies have been adopted to immobilize $TiO_2$, including the direct addition of $TiO_2$ nanoparticles to the membrane casting solution [15,16] and self-assembly of $TiO_2$ through non-covalent interaction, such as electrostatic affinity or coordination interaction, with the surface of the membranes [14,17,18,19,20]. The former endows the membrane with stable mechanical properties yet destructs the membrane morphology due to the agglomeration of $TiO_2$ grains in pores and on the surface that weakens the antifouling ability [18,21]. In contrast, the surface self-assembly method may effectively resolve the aggregation issue, while it highly depends on the surface functional groups which serve as binding sites to fix $TiO_2$ tightly. However, to create surface functional groups require breaking the ultra-stable C-F bonds and activating the intrinsic chemical inertia of PTFE.

Non-thermal plasma represents a promising and environmentally benign strategy to break C-F bond in PTFE because plasma may generate high-energy active species under mild conditions without destroying surface structure. However, it was found that the plasma-activated surface could not be sustained due to the short life span of active species on polymer surface [11,12]. To address this issue, hydroxyl groups have been introduced onto the membrane surface to maintain the active surface acquired from plasma treatments [13]. You and coworkers has employed plasma-grafted poly acrylic acid (PAA) on polyvinylidene difluoride (PVDF) membrane to bind $TiO_2$ strongly since the plasma-grafted PAA can not only bond to plasma-activated PVDF but also offered binding sites to coordinate with $TiO_2$ [19]. The received modified membrane exhibited improved flux behavior after UV radiation as a result of the super hydrophilicity and self-cleaning capability of $TiO_2$. Madaeni et al. [13] modified the surface of PVDF through in-situ polymerization of PAA and $TiO_2$ nanoparticles which remarkably improved the PVDF ultrafiltration and self-cleaning properties. Such composite membranes fabricated applying the “grafting” technique, in which $TiO_2$ was initially functionalized by acrylic acid (AA) monomers following with in situ polymerization of a blend solution. Despite the significant advances in polymer ultrafiltration membranes, very little information is available on the self-assembly of $TiO_2$ on the PTFE membranes, not mentioned to their filtration performance and antifouling properties.

In the present work, surface $TiO_2$ modification of porous PTFE membranes was realized via

plasma-enhanced surface graft of PAA prior to coat $TiO_2$ layer. The modified PTFE-UF membranes were well characterized using scanning electron microscopy (SEM), X-ray diffraction (XRD), Fourier transform infrared spectroscopy (FTIR), X-ray photoelectron spectroscopy (XPS), and pure-water contact angle measurements. The antifouling of bovine serum albumin (BSA) via hydrophilic modification through PAA graft polymerization and $TiO_2$ assembly on PTFE surface, MB removal ability via effect of photodegradation, and self-cleaning property under UV irradiation were investigated.

## 2. Experimental

### 2.1 Materials

Bare PTFE microfiltration membrane, with PET as the substrate and PTFE microfibers to form function surface, and the commercial hydrophilic PTFE membrane were both supplied by Valqua Shanghai Co., Ltd. (China). Ti $(OBu)_4$, acetic acid (AA), potassium persulfate, and bovine serum albumin (BSA; Mw = 67,000 Da) were purchased from Sinopharm Chemical Reagent Co., Ltd. (China). Analytical grade acetic acid, nitric acid, absolute ethanol, and ethylene glycol were obtained from Shanghai Lingfeng Chemical Reagent Co., Ltd. (China). All reagents were used without further purification. Distilled water was used throughout the study.

### 2.2 Membrane modification procedures

A novel modification methodology was developed to modify the PTFE membranes, including the successive 3-step processes: plasma pretreatment of PTFE, graft polymerization of AA onto plasma-treated PTFE to form PAA/PTFE, and $TiO_2$ self-assembly onto the PAA/PTFE to obtain the composite membranes. Briefly, plasma (10 sccm) was generated using a CTP-2000K device (Corona Lab, Nanjing, China) at an excitation frequency of 10 KHz. The clean and dry bare PTFE membranes were treated for 120s in a plasma generator chamber (distance of the plasma electrode of 8mm) in $N_2$ flow under a discharge power of 60 W. The received membranes were then exposed to air for 10 min before in-situ grafting PAA polymer onto the surface. The aqueous solution used in PAA polymerization on membrane surface is the mixture of containing 20 wt.% aqueous AA monomer solution using potassium persulfate (1 wt.%) as initiator and the ethylene glycol (EG) as cross linker with the molar ratio of EG:AA= 1:6.5. The plasma-treated PTFE membrane was immersed in the monomer solution for 5 min and then rolled the residual AA use a clean glass rod for coating PAA evenly. The membrane was then placed between two clean glass plates before being vacuum-dried at 75 °C for 4 h. The grafting step could form an appropriate layer of PAA on the PTFE membrane surface, which is a crucial step because the coated PAA provides $COO^-$ to functional groups that will coordinate with $Ti^{4+}$ to form a tight $TiO_2$ coat in the following step. In the third step, the PAA/PTFE membranes were dipped in $TiO_2$ sol for 20 min to self-assemble $TiO_2$ layers and form the final $TiO_2$/PAA/PTFE membranes[14]. The above mentioned $TiO_2$ sol used in self-assembly was synthesized by mixing solution A and solution B[15]. Solution A was made by dissolving 10 mL tetrabutyl titanate Ti $(OBu)_4$ and 2 mL acetic acid in 30 mL anhydrous ethanol and stirred in a 250 mL flask for 30 min. Solution B was made by adding and completely mixing 0.5 mL nitric acid, 10 mL anhydrous ethanol and 1 mL distilled water in a 250 mL flask. The $TiO_2$ sol formed when slowly adding solution B to solution A drop wise under continuously stirring at room temperature for 1 h until the solution became transparent yellow.

The mass of the PTFE membranes increased during modification, particularly after introducing AA and $TiO_2$ to the surface. The mass gain rate can be calculated by using the following equation:

$$R\,(\%) = \frac{M_t - M_0}{M_0} \quad (1)$$

where R is the mass gain rate, $M_t$ the mass of the treated and dried composite membrane, and $M_0$ the mass of the untreated membrane.

The modification procedures for different membrane samples are listed in Table 1, along with the membranes' mean pore size, mass per unit and mechanical properties.

Table 1 Description of the bare and modified PTFE membranes

| Membrane | Mean pore size (μm) | Mass per unit ($g/m^2$) |
|---|---|---|
| Bare PTFE | 0.50(±0.01) | 88.99(±1.21) |
| Plasma pretreated PTFE | 0.67(±0.02) | 88.99(±1.21) |
| PAA/PTFE | 0.36(±0.01) | 108.57(±1.49) |
| $TiO_2$/PAA/PTFE | 0.22(±0.02) | 130.29(±1.50) |
| Commercial hydrophilic PTFE | 0.30(±0.01) | 91.02(±1.20) |

Note: the numbers in brackets represent measuring errors.

2.3 Surface free radical concentration

In order to determine surface free radical concentration, 1,1-Diphenyl-2-picrylhydrazyl (DPPH) free radical assay was applied in this study. The plasma-treated membrane samples (S = 9 $cm^2$) were exposed to air for 10 min first and then transferred to a brown glass bottle containing DPPH ($1\times10^{-4}$ mol/L) ethanol solution (V = 0.1 L) for 48 h immersion at room temperature under weak light. In this period, the DPPH would react with peroxy radicals at the mole ratio of 2:1 [17]. The free radical concentration ($C_R$) could be calculated from equation (2) shown below, where $C_0$ and $C_1$ are concentrations of DPPH before and post the reaction ($C_1$):

$$C_R = \frac{C_0 - C_1}{S} \times V \quad (2)$$

2.4 Membrane characterization

The surface morphologies of the modified and unmodified membranes were observed on a Sirion 200 E scanning electron microscope. The membranes were treated by desiccation and sprayed gold before SEM observation. The chemistry nature of the membranes was investigated using a Thermo Fisher Nicolet 6700 Fourier transform infrared spectrometer (USA) ， Bruker D8 Advance X-Ray Polycrystaline Diffractometer (German) and Kratos AXIS Ultra DLD X-ray photoelectron spectroscope (Japan). A CAM110 contact angle-measuring device (Taiwan) was used to analyze the surface hydrophilicity.

2.5 Filtration performance

The antifouling property of commercial and self-made modified PTFE membranes was assessed through filtration experiments conducted in a dead-end filtration cell with a total filtration area of 0.0139 $m^2$. The pure water flux was measured at room temperature and under operating pressure of 100KPa after pre-operating for 30 min. The flux of permeate was calculated according to Darcy law described as Eq(3).

$$J_{w0} = \frac{V}{A\Delta t} \quad (3)$$

Where V is the permeate volume (L), A the membrane area (m2), and $\Delta t$ the permeate time (h).

Membrane retention ability was tested using fresh solution of 1g/L BSA in phosphate buffer saline at pH 7.4 at a temperature of 20 °C and under an operating pressure of 0.1 MPa. The concentrations of both the feed water and the permeation water were determined using an ultraviolet spectrophotometer (TU-1810, Beijing Purkinje Genera, China) at a wavelength of 280 nm. The percentage of the observed rejection(R) of BSA solutes in phosphate buffer was calculated as the following Eq.(4):

$R=(1-C_p/C_f)\times 100\%$ (4)

where $C_p$ is the permeate concentration and $C_f$ is the feed concentration.

To investigate fouling property, the sample was fouled for 2 h in the fresh phosphate buffer saline solution containing BSA (1 g/L) at pH 7.4. The water flux during continuous filtration of BSA solution was collected every 30 s, which indicates the decrease of flux during fouling. The pure water flux of the fouled membrane ($J_{w1}$) was measured after 2 hr filtration to reflect the decrease of filtration capability. There was a layer of thick protein cake left on the membrane surface because protein blocked the pores and deposited on the surface. To measure the recovery ability of the membranes, the blocked membranes were rinsed with pure water and illuminated using a 300 W Xe lamp for 15~30min respectively. The pure water flux on the recovered membrane ($J_{w2}$) was then measured to evaluate the performance of the modified membranes.

The relative flux reduction (RFR) and the flux recovery ratio (FRR) were calculated using the following equations

$$RFR = \frac{J_{w0} - J_{w1}}{J_{w0}} \times 100\% \quad (5)$$

$$FRR = \frac{J_{w2}}{J_{w0}} \times 100\% \quad (6)$$

## 2 .6 Photocatalytic degradation of MB

Methylene Blue (MB) was used as a model pollutant to evaluate the photodegradation ability of PTFE/PAA/$TiO_2$ composite membranes under full arc Xe lamp irradiation. The composite membrane with certain area was tailored to unify the $TiO_2$ loading of 10 mg on the membrane, and then immersed 100 mL methylene blue (MB, 10mg/L) aqueous solution in a beaker. The pH of the MB solution was adjusted to neutral (pH=7.0) using dilute sodium hydroxide (NaOH) and chloride acid (HCl). The beaker was positioned directly under full arc irradiation generated by a 300 W Xe lamp (15 cm above the dishes) with a 400 nm cutoff filter as a light source. The MB solution and the $TiO_2$/PAA/PTFE composite membrane were mixed on a magnetic stirring machine and remained in dark for an hour to establish a MB solution adsorption–desorption equilibrium on the membrane before light irradiation. During photocatalysis, 4 mL reaction solution was taken out every 15 min and filtered so as to measure the concentration change of MB using a UV-visible spectrophotometer (Perkinelmer, Lambda 650, USA).

For comparison, the photodegradation of MB on bare PTFE membrane was also conducted using the same method. Since the MB aqueous solution was at rather low concentration, its photodegradation followed a pseudo first-order reaction and its kinetics can be expressed as

$$-\ln\left(\frac{C}{C_0}\right) = kt \quad (7)$$

where $C_0$ (mg/L) is the initial MB concentration, C (mg/L) is the MB concentrations after certain irradiation time, t (min) is the irradiation duration in minute while sampling, k (min-1) reflects the reaction rate constant and its values are derived from the slopes of the linear curves of $-\ln(C/C_0)$ versus irradiation time t.

## 3. Results and discussion

### 3.1 Membrane modification mechanism

As pretreatment, plasma is necessary not only to produce several functional groups on the hydrophobic surface of bare PTFE membranes, but also to generate numerous activated species such as highly active alkyl radicals which are prone to quenching in air. When exposed to air, alkyl radicals are stabilized by reacting with oxygen and moisture to generate relatively stable carboxyl and peroxyl radicals on the membrane surface due to their special resonance structures [16], leading to improved surface wettability. The as-formed radicals would act as initiator for sequential surface graft of PAA. The concentration of surface free radical was measured to be $1.17\times10^{-7}$ mol/cm2 in our study. This result showed that peroxyl radicals could be formed under the operating parameters of plasma treatment. When high energy-activated species, such as electrons, radicals, and ions contained in plasmas, the C-F and C-C bonds of the PTFE material would be broken. The optimization of plasma operation is not the focus of this study and would discuss in details later.

The surface morphology evolution of PTFE membranes with respective to the modification process was investigated by SEM and the obtained images of the membranes are shown in Fig.1. Fig. 1a shows the SEM image of the plasma treated PTFE membrane which is similar to that of bare PTFE membrane because of short treatment duration. It can be seen there are PTFE microfibers with uniform diameter interweaved and forming multi-scale pores randomly dispersed on the surface of plasma-treated PTFE membrane. The surface graft of PAA did not change the fibrous morphology of PTFE membrane (Fig. 1b), while significantly changed the surface roughness and reduced the surface porosity of the PTFE membrane. The surface of PTFE fibers cannot be observed in the SEM images of $TiO_2$/PAA/PTFE (Fig. 1c and d). The surface of $TiO_2$/PAA/PTFE is relatively smooth (Fig. 1c) compared to bare PTFE and PAA/PTFE membranes, revealing the $TiO_2$ was immobilized and well deposited on the surface of the plasma-assisted PAA/PTFE membrane to form a dense and continuous surface layer of $TiO_2$. The observation of the composite membrane by high resolution SEM (Fig. 1d) shows the $TiO_2$ layer is composed of ultrafine nanoparticles except for small $TiO_2$ aggregates (diameter in 0.2~0.3 μm) randomly anchored on the surface of the composite membrane, while there are smaller pores existing on the $TiO_2$ layer which would allow the water penetration yet influence the pressure drop in the ultrafiltration application.

The mass of the bare and modified PTFE membranes was measured during the modification process (Table 1), which could be used as the physical evidence of PAA and TiO2 functional layers bonding to the bare PTFE membranes. After graft polymerization of AA, the mass of the PTFE membrane increased

by 12%, while the self-assembly of $TiO_2$ caused further 9% increase.

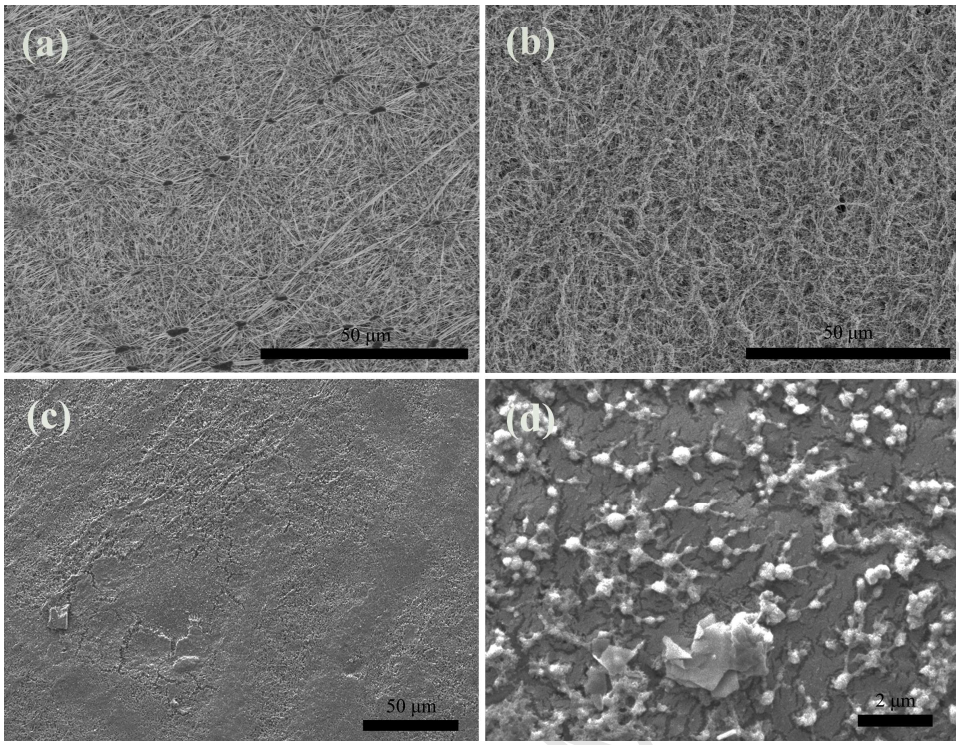


Fig. 1. SEM images of bare PTFE and composite-modified PTFE membranes:
(a) Plasma pretreated PTFE (×1k), (b) PAA/PTFE (×1k), (c) $TiO_2$/PAA/PTFE (×1k), (d) $TiO_2$/PAA/PTFE (×20k)

In order to further verify the success of modification and to propose chemical mechanism of the PTFE modification process, XRD, XPS, FTIR were used to compare the difference among bare PTFE membranes, PAA/PTFE membrane and $TiO_2$/PAA/PTFE membranes.

The XRD measurements were employed to examine the crystalline phase of the bare PTFE membrane, PAA/PTFE composite membrane, and $TiO_2$/PAA/PTFE composite membrane, and the diffraction spectra were shown in Fig.2 (a). It was observed that there were three dominated crystalline peaks for bare PTFE membranes (with PET as substrate). The first peaks at 2θ angle of 18.3 were from PTFE, the other two peaks at 22.80º and 26.00º correspond to the (100) and (200) diffractions of PET substrate [22]. The reduced intensity of the crystalline peaks as PAA grafted onto PTFE membranes implied that the crystalline region within PTFE membrane was destroyed and the amorphous phase was slightly enhanced due to the interaction between PAA and PTFE polymers. The slight shift of the diffraction spectra for PAA/PTFE membranes compared to bare PTFE membrane also confirmed that there was a strong interaction between the grafted PAA layer and the bare PTFE membranes. The shoulder peaks around the main diffractions at 18.03 $^{o}$ and 25.8 $^{o}$ were observed in spectra of PAA/PTFE membranes and TiO2/PAA/PTFE membranes, which were attributed to the overlapping diffractions of PAA and $TiO_2$ with PTFE and PET[23]. The overlapping of $TiO_2$ diffractions with PTFE and PET can be clearly verified by comparing the XRD pattern of pure anatase $TiO_2$ with the composite membranes. In the pattern of the pure anatase $TiO_2$ (prepared by drying the $TiO_2$ sol at 60 ºC followed by calcinations at

500 ºC/2 h), the diffraction peaks at 25.2 º, 37.1 º, 48.2 º correspond to the (101), (004), and (200) crystal faces of $TiO_2$ respectively (JCPDS 71-1169). The peak shifts in XRD pattern of $TiO_2$/PAA/PTFE composite membrane suggest the $TiO_2$ has been coated onto PAA/PTFE membranes with strong interactions due to the chemical bonding between $TiO_2$ and the PAA/PTFE substrates. The strong interactions between TiO2 and PAA/PTFE membranes due to TiO2 coating could also be verified by the enhanced intensity of the crystalline peaks for TiO2/PAA/PTFE membranes.

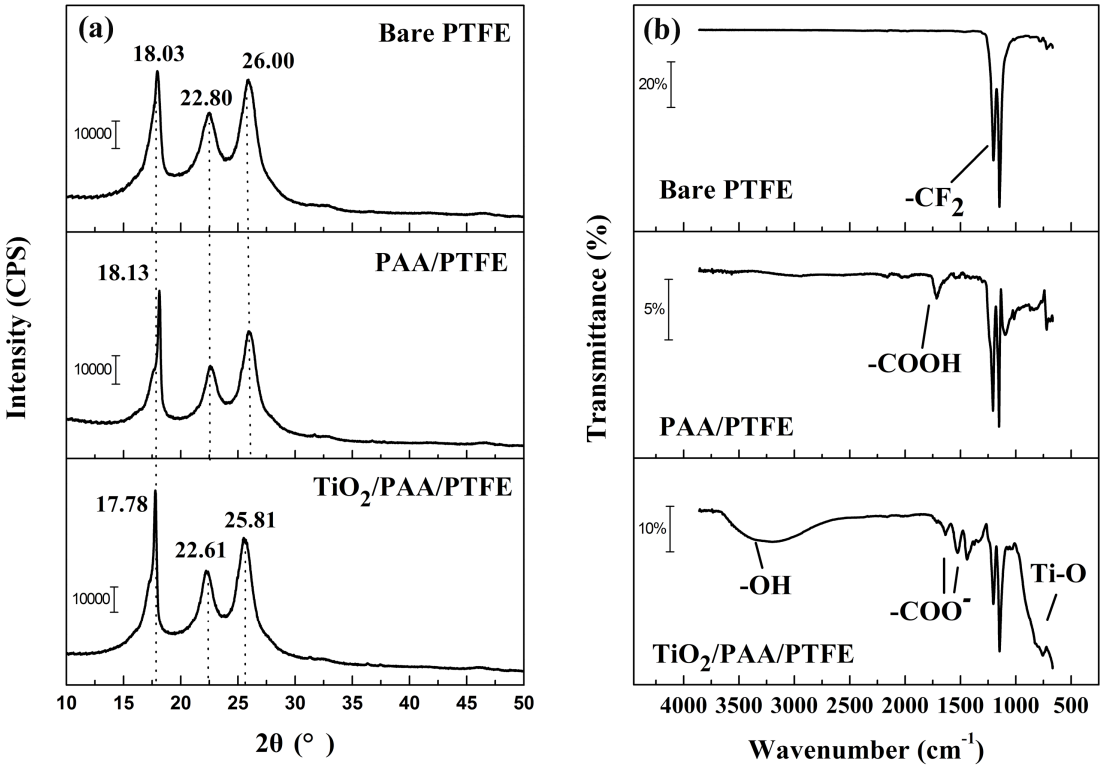


Fig. 2. （a）XRD patterns and (b) ATR-FTIR spectra of bare PTFE, PAA/PTFE, $TiO_2$/PAA/PTFE composite membranes

Attenuated total reflection flourier transition infrared spectroscopy (ATR-FTIR) was used to characterize the surface functional groups on the PTFE and the modified PTFE membranes and the results were shown in Fig. 2(b). Only two strong vibration absorption peaks at 1201 $cm^{-1}$ and 1148 $cm^{-1}$ associated to $CF_2$ absorption were observed on the bare PTFE membrane [18], while a new peak at 1715 $cm^{-1}$ was observed on the PAA/PTFE composite membrane, which is attributed to the C=O bond stretching in the carboxyl group, suggesting the successful graft of PAA [13].

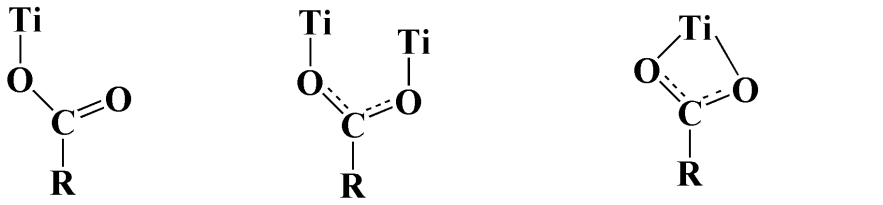


**(A) Monodentate** **(B) Bridging Bidentate** **(C) Chelating Bidentate**

Fig. 3. The three coordination modes of $RCOO^-$ and $Ti^{4+}$ cation

In the ATR-FTIR spectra of the $TiO_2$/PAA/PTFE membrane, besides the vibration of CF2, the strong and broad absorption band appeared in the region within 600 -800 $cm^{-1}$ may be attributed to the stretching vibration of Ti-O-Ti and Ti-O bonds in $TiO_2$ [13], revealing that $TiO_2$ had been immobilized on the PAA/PTFE membrane surface post the self-assembly coating. The broad and weak stretching vibration band around 3200 $cm^{-1}$ may be assigned to Ti-OH and surface-adsorbed water [19]. In comparison to the ATR-FTIR of PAA/PTFE, the peak of the C=O group at 1715 $cm^{-1}$ is much weaker yet two rather stronger transformation vibrations attributed to C-O bonds were observed within 1610 ~1360 $cm^{-1}$ region. These C-O vibration spectra can be assigned to the coordination between $Ti^{4+}$ and carboxyl group ($COO^-$). The vibration bands in the 1610 ~1520 $cm^{-1}$ and 1440~1360 $cm^{-1}$ regions correspond to the antisymmetric ($V_{as}$) and symmetric ($V_s$) stretching vibrations modes of the titanium carboxylates, respectively. In principle [21], there are three coordination configurations between $Ti^{4+}$ and $COO^-$, including monodentate, bridging bidentate, and chelating bidentate, as shown in Fig. 3. The exact coordination mode of $COO^-$-Ti can be identified by comparing the FTIR wavenumber difference between $COO^-$-Ti ($\Delta V_c$) and that of $COO^-$Na ($\Delta V_0$, ~165 $cm^-$ ) in the FTIR spectra. $\Delta V_c$ and $\Delta V_0$ are defined using the following expressions.

$$\Delta V_c = V_{as}(COO^- - Ti) - V_s(COO^- - Ti)$$

$$\Delta V_0 = V_{as}(COO^- - Na) - V_s(COO^- - Na) \quad (8)$$

For monodentate structure, $\Delta V_c > \Delta V_0$; for bridging bidentate structure, $\Delta V_c \approx \Delta V_0$;for chelating bidentate structure, $\Delta V_c < \Delta V_0$ [20]. The relevant wavenumber data of $V_{as}$, $V_s$ and $\Delta V_0$ were listed in Table 2. It was found that the $\Delta V_c$ in this work is smaller than $\Delta V_0$, suggesting that $TiO_2$ is coated on the PAA/PTFE through the bidentate chelating coordination between $Ti^{4+}$ and carboxyl groups.

Table 2 Vibration wavenumber of carboxylate anion

| | $V_{as}(COO^-)$/$cm^{-1}$ | $V_s(COO^-)$/$cm^{-1}$ | $V_{as} - V_s$ ($cm^{-1}$) |
|---|---|---|---|
| $COO^-$-Na | 1573 | 1408 | 165 ($\Delta V_0$) |

| | | | |
|---|---|---|---|
| $COO^-$-Ti | 1525 | 1374 | 151 ($\Delta V_c$) |

The surface chemical species of the bare and modified PTFE membranes were characterized using XPS shown in Fig. 4. It can be seen that all the bare and modified PTFE-based ultrafiltration membranes exhibit the characteristic C1s and F1s XPS within PTFE at 292.3 eV and 687.1 eV, respectively (Fig. 4a). However, the intensity of the C1s and F1s XPS of the $TiO_2$/PAA/PTFE is much weaker than those of PTFE and plasma-treated PTFE, indicating the $TiO_2$ layer well covered the composite membrane and thus reduced the exposure of PTFE surface. It is worth noting the O1s (531.6 eV) is clearly observed in the XPS survey spectra of the PTFE with plasma pretreatment and air-exposure, though the C1s and F1s XPS peaks dominate the XPS survey spectra of bare and the pretreated PTFE membranes. The results suggest the plasma combined with air exposure leading to the formation of significant amount of tightly bonded oxygen species on the PTFE. The O1s intensity is further increased once $TiO_2$ was coated onto the PAA/PTFE membrane due to the increased amount of O species amount relative to PAA and $TiO_2$. Moreover, the Ti2p XPS peak centering at 464.7 eV were observed on the survey spectra of $TiO_2$/PAA/PTFE membrane, confirming the $TiO_2$ was successfully loaded on the modified PTFE UF membrane. The $TiO_2$ loading is therefore responsible for the weaker C1s and F1s XPS spectra in $TiO_2$/PAA/PTFE than those of bare and plasma-treated PTFE membranes. The quantitative surface chemical composition of the bare and modified PTFE membranes was compared in Table 3, from which the gradual variation of the concentration of surface C, F and O species clearly. This verifies the successful immobilization of $TiO_2$ onto the PAA/PTFE membranes, suggesting that the plasma-induced graft of PAA is an effective pretreatment methodology for coating $TiO_2$ onto PTFE.

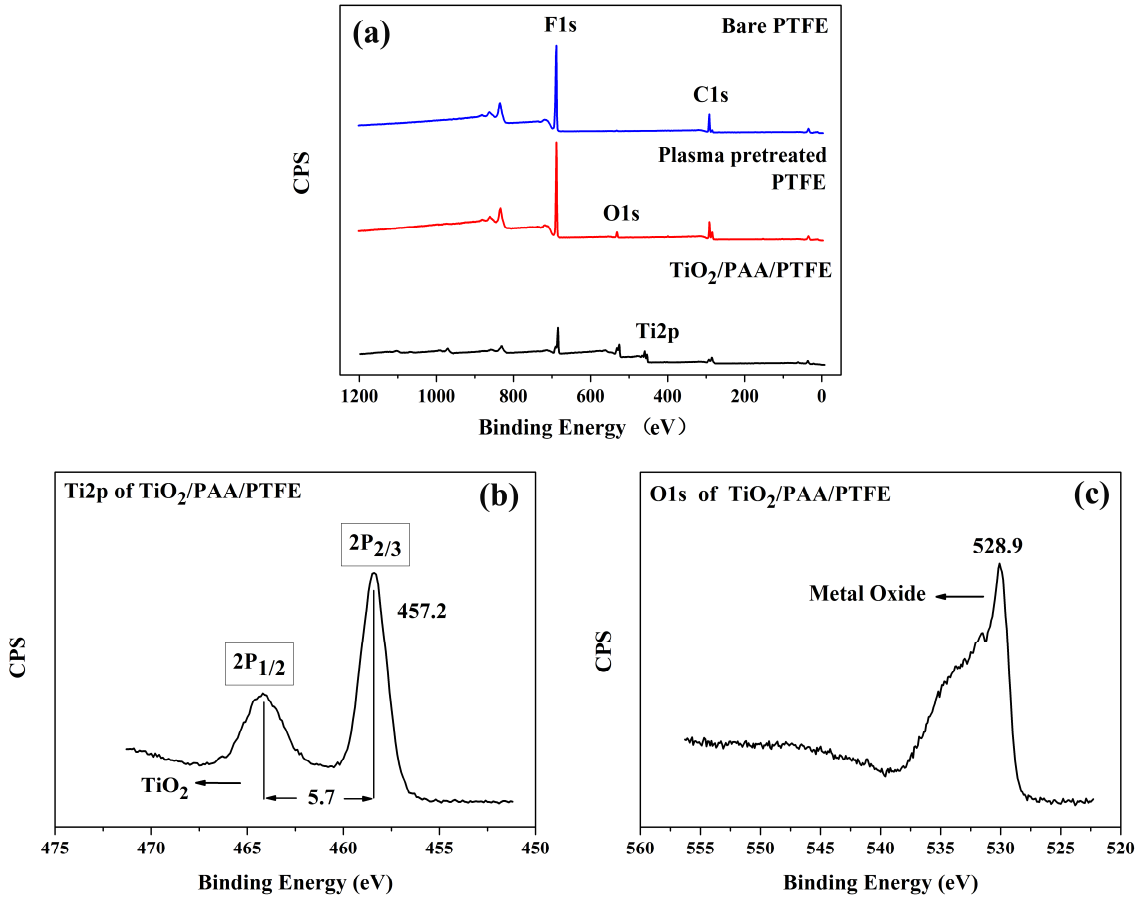


Fig. 4. (a) The XPS survey spectra of the bare and modified PTFE-based ultrafiltration membranes; (b) high resolution Ti2p XPS spectra; (c) high resolution O1s XPS spectra

Fig. 4b shows the high resolution Ti2p XPS spectra, where the $Ti2p_{1/2}$ (462.9 eV) and $Ti2p_{3/2}$ (457.2 eV) are clearly split with the binding energy difference at 5.7 eV, which accords with the Ti XPS in $TiO_2$ reported in literature [24,25]. In the high resolution O1s XPS spectra of $TiO_2$/PAA/PTFE (Fig. 4c), the major peak centering at 528.9 eV may be assigned to the O species in the $TiO_2$, while the large and broad shoulder peak may be attributed to the O species in PAA.

Table 3 Surface composition of untreated and treated PTFE membranes measured by XPS

| Membrane sample | Atomic percentage/% | | | | Elemental ratios | |
|---|---|---|---|---|---|---|
| | F | C | O | Ti | F/C | O/C |
| Bare PTFE | 91.86 | 7.01 | 1.13 | -- | 13.10 | 0.16 |
| Plasma treated PTFE | 84.20 | 10.91 | 4.85 | -- | 7.72 | 0.44 |
| PAA/PTFE | 77.36 | 11.92 | 10.72 | -- | 6.49 | 0.90 |
| $TiO_2$/PAA/PTFE | 41.33 | 21.60 | 28.29 | 8.79 | 1.91 | 1.31 |

The preceding experiment results demonstrated that $TiO_2$ can be stably immobilized on the surface of the PTFE membrane through successive 3-step treatments: plasma treatment, graft polymerization of AA, and self-assembly of $TiO_2$. These procedures can well interpret reaction mechanisms. As illustrated in Fig. 5, a 3-step successive reaction protocol can be reasonably proposed to interpret the coating

mechanism. First, the strong C-F and C-C bonds of the PTFE material were broken by active species during plasma treatment, thus generating free radicals on the membrane surface. Once the membrane was exposed to air, relatively stable peroxy radicals formed. These highly reactive groups functioned as initiators of the graft polymerization of AA. The PAA layer provided sufficient binding sites for $TiO_2$, which facilitated the coordination between Ti ion and the carboxyl group through three possible modes (Fig.3). In the present study, $TiO_2$ was immobilized on the PTFE surface through chelating bidentate coordination mode, as indicated by the result of the FTIR analysis.

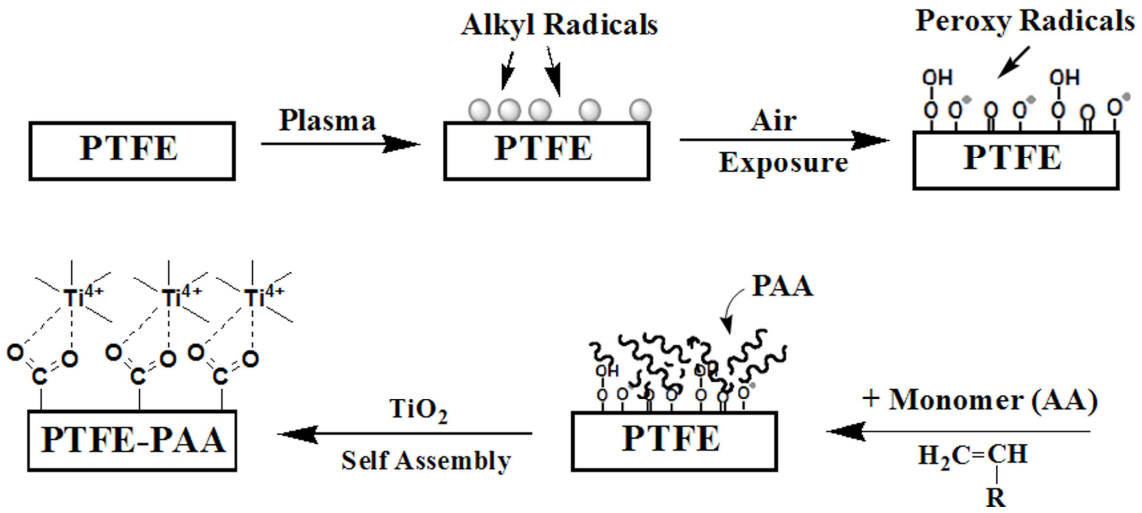


Fig. 5. Mechanism of the plasma-induced graft polymerization of PAA and the self-assembly of $TiO_2$ on the PTFE membrane

3.2 Multi-function of modified membranes

3.2.1 Surface hydrophilicity

The surface hydrophilicity is a crucial factor determining water flux performance of ultrafiltration membranes since high flux requires excellent hydrophilicity. The sessile drop method was adopted to measure the water contact angles on the bare and modified PTFE membranes to compare their surface hydrophilicity and the results are presented in Fig. 6. The water contact angle of the bare hydrophobic PTFE membrane (M0) is around 115.8 °. The contact angle drops down to 99.5 $^{o}$ after air plasma treatment of the PTFE membrane, which can be further reduced to 81.9 $^{o}$ once coating PAA onto PTFE. Although both the plasma and PAA treatments may promote the hydrophilicity of PTFE (with approximately 18 $^{o}$ contact angles drops, respectively), coating with $TiO_2$ dramatically decreased the water contact angle down to 35 °. The results suggest the $TiO_2$ layer plays crucial roles in reducing the water contact angle, namely the improvement of wettability.

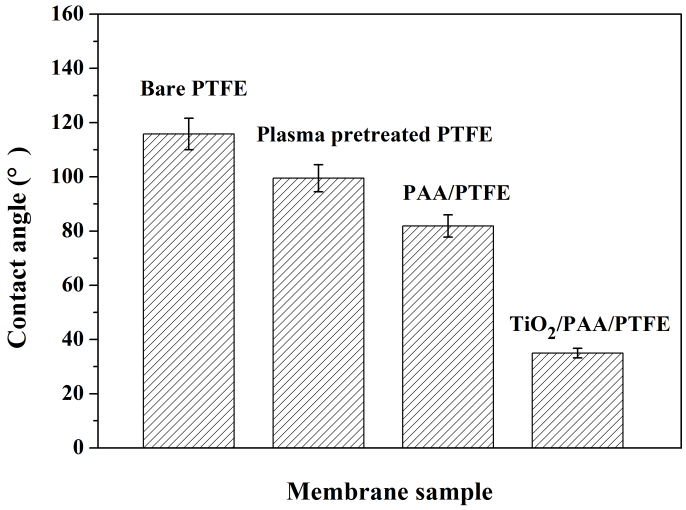


Fig. 6. Water contact angles on bare and modified PTFE membranes

A 30-day cycling test was conducted by immersing the membranes in pure water bath at room temperature under vigorous stirring to check the durability of the hydrophilic modification. The evolution of contact angle with respective to the immersing duration was plotted in Fig. 7. The contact angles of the plasma-treated PTFE membrane and the PAA/PTFE membrane increased significantly in 5-day operation, revealing their hydrophobicity was largely recovered. The wettability of plasma-treated PTFE approached to that of bare PTFE after 5-day test, indicating plasma technique may only temporarily modify the PTFE surface because plasma-induced surface hydrophilic species are not stable and necessitate stabilizer to maintain the derived hydrophilicity. The recovery of the hydrophobicity of PAA/PTFE was supposed to be caused by the mobility of the molecular chain segment or the aging of polymer on the sample surface upon exposing to air after plasma treatment [26].

Although the water contact angle on PAA/PTFE membrane was also increased, it is still $20^{o}$ smaller than that on PTFE after 5 day treatment and remains unchanged in the onwards operation, revealing the PAA possesses excellent coating stability and higher intrinsic hydrophilicity than PTFE. The results convinced PAA surface graft is good solution to improve the surface hydrophilicity of PTFE in that PAA can stabilize or transform the plasma-induced surface hydrophilic species on PTFE. The variation of the water contact angle on the $TiO_2$/PAA/PTFE membrane trended to be constant, around $40^{o}$, only a slight increase to the initial value. The stable hydrophilicity of $TiO_2$/PAA/PTFE in long time operation suggests $TiO_2$ was tightly attached onto PAA/PTFE while the negligible initial increase of contact angle is due to falling off a small portion of unstably immobilized $TiO_2$. Therefore, it can be concluded that the 3-step modification procedure is very effective as verified by the stable hydrophilicity displayed on the $TiO_2$-modified PTFE composite membrane.

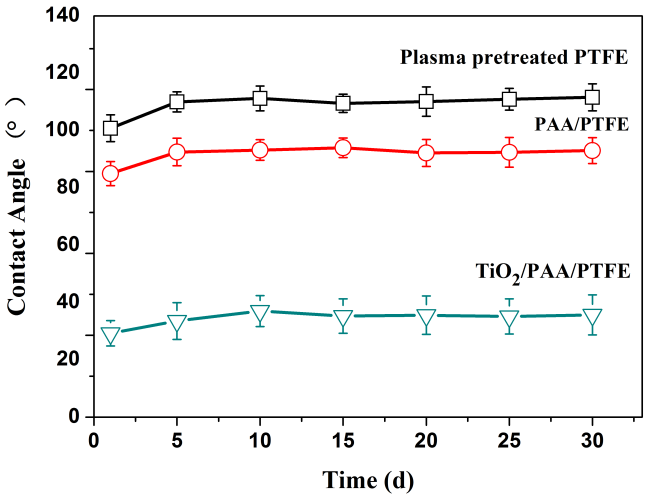


Fig. 7. Comparison of the water contact angles of different PTFE-modified membranes

3.2.2 Antifouling performance

The water flux of the $TiO_2$/PAA/PTFE composite membrane and commercial hydrophilic PTFE were monitored during continuous filtration of 1000 ppm BSA solution. As shown in Fig. 8, the water flux of commercial hydrophilic PTFE membrane demonstrated a sharp decline in the initial 20 min and its high original flux almost vanished; meanwhile its BSA retention rate was only 35% at the steady stage, unsuitable for protein filtration. In contrast, $TiO_2$/PAA/PTFE composite membrane exhibited much slower flux decay in the BSA filtration test and the steady stage water flux is 4 times that on commercial PTFE ultrafiltration membrane, more importantly, its retention rate remained 72% at the steady filtration stage. The results suggest the modification strategy is very effective to resist protein-induced fouling because the $TiO_2$ possesses abundant surface hydroxyl groups which are more hydrophilic and thus weakening the adsorption and attachment of the hydrophobic pollutants, such as protein and bacterium.

3.2.3 Regeneration and photocatalytic self-cleaning performance

Manual washing and UV assisted washing methods were applied to clean the BSA-fouled commercial and modified PTFE UF membranes to recover their water flux. Their flux recovery performance was evaluated using relative flux reduction (RFR) and the flux recovery ratio (FRR) as indexes, as compared in Table 4. It can be seen that FRR ratios derived from manual washing and RFR ratios for $TiO_2$/PAA/PTFE, PAA/PTFE and the commercial PTFE UF membranes are very similar, suggesting the $TiO_2$ modification itself cannot offer self-cleaning property. However, after exposure to UV radiation for 15 min during washing, the FRR of $TiO_2$/PAA/PTFE reached 82%, much better than the PAA/PTFE and commercial PTFE UF membranes. Once extending the UV-assisted washing to 30 min, the $TiO_2$/PAA/PTFE membrane fully recovered its initial water flux, PAA/PTFE and the commercial PTFE UF membranes only gained relatively lower FRRs. It is noticeable the UV-irradiation may enhance the FRRs for all the UF membranes because UV may partly degrade protein and thus weaken their binding to UF membranes. The results suggest that UV-irradiation triggers the self-cleaning performance of the membranes while it is the coated $TiO_2$ that dramatically enhanced the self-cleaning capability of the $TiO_2$/PAA/PTFE.

The enhanced FRR of the $TiO_2$/PAA/PTFE membrane under UV irradiation can be attributed to the photocatalytic surface self-cleaning property of $TiO_2$. On the one hand, under UV light irradiation, the photogenerated excitons (electrons and holes) on $TiO_2$ may react with water molecules and dissolved oxygen to generate reactive radicals that may break chemical bonds binding protein and the membrane surface, resulting in enhanced water resining performance [13,27,28]. On the other hand, the photogenerated excitons may react with the surface-adsorbed water to form superhydorphilic surface hydroxyl (–OH) groups [29]. The hydrophilic surface –OH groups are repelling protein and thus facilitate washing them off. Therefore, it is reasonable to conclude that the photocatalysis property of $TiO_2$ layer is responsible for much higher FRR than PAA/PTFE and commercial PTFE membranes in the UV-assisted washing regeneration.

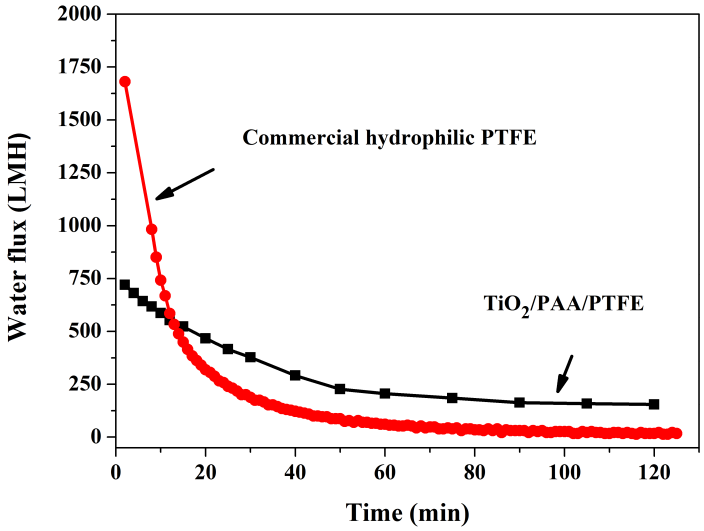


Fig. 8. Variations in flux of the two kinds of PTFE hydrophilic modified membranes during the filtration of 1 g/L BSA (0.1 MPa)

Table 4 Antifouling performances of the commercial and self-made PTFE modified membranes

| Membrane | Water flux ($L•m^{-2}•h^{-1}$) | RFR (%) | FRR (%) | | |
|---|---|---|---|---|---|
| | | | Water rinsing | UV 15 min | UV 30 min |
| PAA/PTFE | 921.43(±10.68) | 81.12(±1.12) | 27.52(±1.10) | 59.00(±1.52) | 76.28(±1.37) |
| $TiO_2$/PAA/PTFE | 848.57(±12.93) | 86.40(±1.33) | 30.27(±1.43) | 82.97(±1.60) | 99.29(±1.55) |
| Commercial hydrophilic PTFE | 1945.70(±15.11) | 77.30(±0.99) | 27.71(±1.02) | 37.66(±1.21) | 53.42(±1.39) |

Note: the error bar was enclosed in the brackets.

In order to further verify the photocatalysis-induced self-cleaning function of $TiO_2$/PAA/PTFE composite membranes and validate the proposed photocatalytic self-cleaning mechanism, photodegradation of methylene blue (MB) was conducted on the PTFE and $TiO_2$/PAA/PTFE membranes. As shown in Fig. 9 (a), the composite membrane exhibited superb photocatalystic activity in photodegradation of MB which decomposed more than 90% MB after 100 min illumination, while only less than 5% MB removal efficiency was observed over the bare PTFE membrane. The high degradation ability of the composite

membrane can be assigned to the excellent photocatalytic property of $TiO_2$ coating, on which photo-active redox species may be excited by UV-light and thus decompose the adsorbed organic pollutant. The photo-active species are typically superoxide radicals formed by the excited electrons reacting with dissolved $O_2$, while the photogenerated holes would react with water to generate highly reactive hydroxyl radicals, ·OH [30].

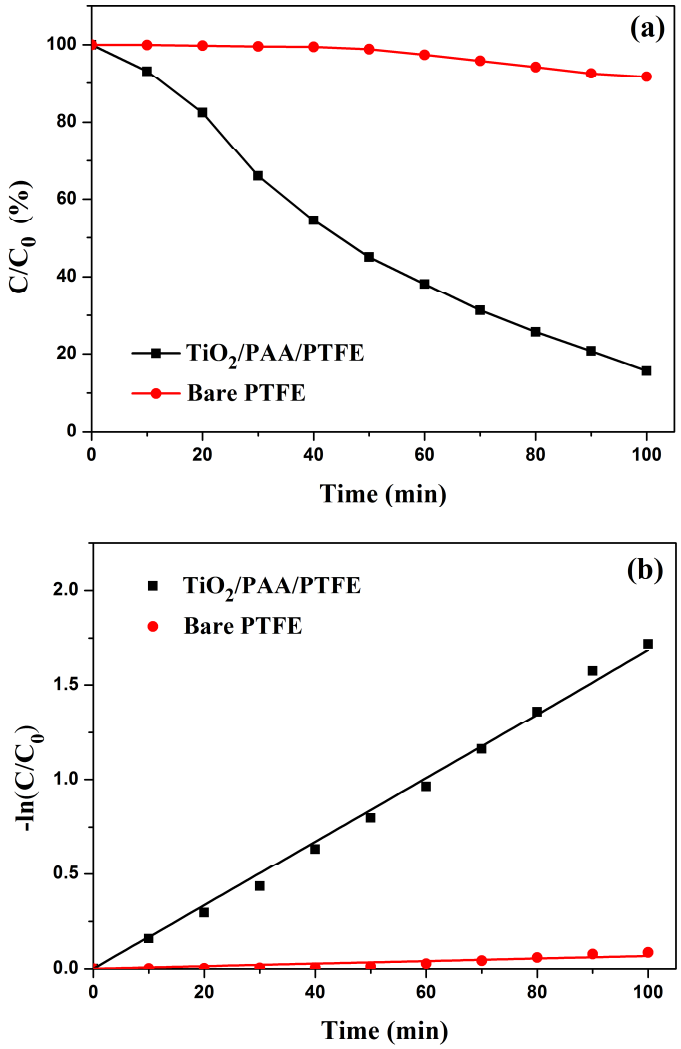


Fig.9 (a) photocatalytic degradation of MB under UV-visible light irradiation, (b) linear transform ln ($C_0$/C) of kinetic curves of MB degradation

Fig. 9 (b) presents the kinetics plots of MB photodegradation on PTFE and $TiO_2$/PAA/PTFE. The linear kinetics plots suggests that the photodegradation reaction of MB on $TiO_2$-modified PTFE follows pseudo-first-order kinetic law. The apparent kinetic constant, k of $TiO_2$/PAA/PTFE composite membrane is 0.0187, approximately 20 times that of bare PTFE (0.0009 $min^{-1}$). The results confirm the coated $TiO_2$ offers PTFE membrane excellent photocatalytic activity and justify the modification is a promising strategy to develop self-cleaning UF membranes for water purification.

## 4. Conclusion

We established an effective and novel strategy to fabricate high performance $TiO_2$/PAA/PTFE ultrafiltration membrane via tight coating of $TiO_2$ functional layer onto the plasma-assisted graft of PAA

on PTFE. The thorough experimental characterizations unraveled that the formation of COO-Ti bidentate coordination between $TiO_2$ and PAA is responsible for the successful coating of $TiO_2$ onto PTFE-based polymer ultrafiltration membrane. The $TiO_2$ modification dramatically reduced the water contact angle of PTFE from 115.8 ° to 35 ° and the $TiO_2$/PAA/PTFE membrane exhibited outstanding ultrafiltration stability in 30-day continuous water ultrafiltration operation, while plasma treatment and PAA graft may only improve the surface hydrophilicity of PTFE for short time. The high water flux rate, enhanced ultrafiltration performance, and excellent self-cleaning ability of the as-prepared $TiO_2$/PAA/PTFE membrane were attributed to the intrinsic hydrophilicity and photocatalytic property of $TiO_2$ functional layer.

## Acknowledgement

We acknowledge financial support from Shanghai Jiao Tong University, China, Shanghai Lee's FUDA electromechanical Co.Ltd., China and the Newton Research Collaboration Award from Royal Academy of Engineering, UK (Reference: NRCP/1415/261). We also thank researchers in R&D Department in Shanghai VALQUA Company Limited for their kind supply of bare hydrophobic PTFE membranes and commercial hydrophilic PTFE membranes.

## References

[1] H. Chen, Q. Lin, Q. Xu, Y. Yang, Z. Shao, Y. Wang, Plasma activation and atomic layer deposition of $TiO_2$ on polypropylene membranes for improved performances of lithium-ion batteries, Journal of Membrane Science, 458 (2014) 217-224.

[2] Z. Q. Dong, X. h. Ma, Z. L. Xu, W. T. You, F. b. Li, Superhydrophobic PVDF–PTFE electrospun nanofibrous membranes for desalination by vacuum membrane distillation, Desalination, 347 (2014) 175-183.

[3] S. Bamperng, T. Suwannachart, S. Atchariyawut, R. Jiraratananon, Ozonation of dye wastewater by membrane contactor using PVDF and PTFE membranes, Separation and Purification Technology, 72 (2010) 186-193.

[4] C.V. Amanchukwu, J.R. Harding, Y. Shao-Horn, P.T. Hammond, Understanding the Chemical Stability of Polymers for Lithium–Air Batteries, Chem Mater, 27 (2015) 550-561.

[5] C. H. Yu, I. Kusumawardhana, J. Y. Lai, Y. L. Liu, PTFE/polyamide thin-film composite membranes using PTFE films modified with ethylene diamine polymer and interfacial polymerization: Preparation and pervaporation application, J Colloid Interf Sci, 336 (2009) 260-267.

[6] P. Roy Chaudhury, B.S. Kelly, M. Melhem, J. Zhang, J. Li, P. Desai, R. Munda, S.C. Heffelfinger, Novel Therapies for Hemodialysis Vascular Access Dysfunction: Fact or Fiction!, Blood Purificat, 23 (2005) 29-35.

[7] A. Lin, S. Shao, H. Li, D. Yang, Y. Kong, Preparation and characterization of a new negatively charged polytetrafluoroethylene membrane for treating oilfield wastewater, Journal of Membrane Science, 371 (2011) 286-292.

[8] Q. Xu, Y. Yang, X. Wang, Z. Wang, W. Jin, J. Huang, Y. Wang, Atomic layer deposition of alumina on porous polytetrafluoroethylene membranes for enhanced hydrophilicity and separation performances, Journal of Membrane Science, 415–416 (2012) 435-443.

[9] N. Peng, N. Widjojo, P. Sukitpaneenit, M.M. Teoh, G.G. Lipscomb, T.-S. Chung, J. Y. Lai, Evolution of polymeric hollow fibers as sustainable technologies: Past, present, and future, Progress in Polymer Science, 37 (2012) 1401-1424.

[10] H. Tang, M. Pan, S.P. Jiang, X. Wang, Y. Ruan, Fabrication and characterization of PFSI/ePTFE composite proton exchange membranes of polymer electrolyte fuel cells, Electrochim Acta, 52 (2007)

5304-5311.
[11] C. Bi, H. Zhang, S. Xiao, Y. Zhang, Z. Mai, X. Li, Grafted porous PTFE/partially fluorinated sulfonated poly(arylene ether ketone) composite membrane for PEMFC applications, Journal of Membrane Science, 376 (2011) 170-178.
[12] Z. Jie, T. Haolin, P. Mu, Fabrication and characterization of self-assembled Nafion–$SiO_2$–ePTFE composite membrane of PEM fuel cell, Journal of Membrane Science, 312 (2008) 41-47.
[13] S.S. Madaeni, S. Zinadini, V. Vatanpour, A new approach to improve antifouling property of PVDF membrane using in situ polymerization of PAA functionalized $TiO_2$ nanoparticles, Journal of Membrane Science, 380 (2011) 155-162.
[14] K. Fischer, M. Grimm, J. Meyers, C. Dietrich, R. Gläser, A. Schulze, Photoactive microfiltration membranes via directed synthesis of $TiO_2$ nanoparticles on the polymer surface for removal of drugs from water, Journal of Membrane Science, 478 (2015) 49-57.
[15] J. Wang, J. Huang, H. Xie, A. Qu, Synthesis of g-$C_3N_4$/$TiO_2$ with enhanced photocatalytic activity for H2 evolution by a simple method, Int J Hydrogen Energ, 39 (2014) 6354-6363.
[16] C. Wang, J. R. Chen, Studies on surface graft polymerization of acrylic acid onto PTFE film by remote argon plasma initiation, Appl Surf Sci, 253 (2007) 4599-4606.
[17] J. P. Chen, Y. P. Chiang, Surface modification of non-woven fabric by DC pulsed plasma treatment and graft polymerization with acrylic acid, Journal of Membrane Science, 270 (2006) 212-220.
[18] J. Qiu, J. Ni, M. Zhai, J. Peng, H. Zhou, J. Li, G. Wei, Radiation grafting of styrene and maleic anhydride onto PTFE membranes and sequent sulfonation for applications of vanadium redox battery, Radiat Phys Chem, 76 (2007) 1703-1707.
[19] S. J. You, G.U. Semblante, S. C. Lu, R.A. Damodar, T. C. Wei, Evaluation of the antifouling and photocatalytic properties of poly(vinylidene fluoride) plasma-grafted poly(acrylic acid) membrane with self-assembled $TiO_2$, J Hazard Mater, 237–238 (2012) 10-19.
[20] M. Nara, H. Morii, M. Tanokura, Coordination to divalent cations by calcium-binding proteins studied by FTIR spectroscopy, Biochimica et Biophysica Acta (BBA) - Biomembranes, 1828 (2013) 2319-2327.
[21] B. Hojjati, R. Sui, P.A. Charpentier, Synthesis of $TiO_2$/PAA nanocomposite by RAFT polymerization, Polymer, 48 (2007) 5850-5858.
[22] S. Fernández, A. Martínez-Steele, J.J. Gandía, F.B. Naranjo, Radio frequency sputter deposition of high-quality conductive and transparent ZnO:Al films on polymer substrates for thin film solar cells applications, Thin Solid Films, 517 (2009) 3152-3156.
[23] S. Bekin, S. Sarmad, K. Gürkan, G. Keçeli, G. Gürdağ, Synthesis, characterization and bending behavior of electro responsive sodium alginate/poly(acrylic acid) interpenetrating network films under an electric field stimulus, Sensors and Actuators B: Chemical, 202 (2014) 878-892.
[24] P.M. Kumar, S. Badrinarayanan, M. Sastry, Nanocrystalline $TiO_2$ studied by optical, FTIR and X-ray photoelectron spectroscopy: correlation to presence of surface states, Thin Solid Films, 358 (2000) 122-130.
[25] D. Briggs, Handbook of X-ray Photoelectron Spectroscopy C. D. Wanger, W. M. Riggs, L. E. Davis, J. F. Moulder and G. E.Muilenberg Perkin-Elmer Corp., Physical Electronics Division, Eden Prairie, Minnesota, USA, 1979. 190 pp. 195, Surf. Interface Anal. 3 (1981) v–v.
[26] H. H. Chien, K. J. Ma, C. H. Kuo, S. W. Huang, Effects of plasma power and reaction gases on the surface properties of ePTFE materials during a plasma modification process, Surface and Coatings Technology, 228, Supplement 1 (2013) S477-S481.

595 [27] Y. Mansourpanah, S.S. Madaeni, A. Rahimpour, A. Farhadian, A.H. Taheri, Formation of appropriate
596 sites on nanofiltration membrane surface for binding $TiO_2$ photo-catalyst: Performance,
597 characterization and fouling-resistant capability, Journal of Membrane Science, 330 (2009) 297-306.
598 [28] S.S. Madaeni, N. Ghaemi, Characterization of self-cleaning RO membranes coated with $TiO_2$
599 particles under UV irradiation, Journal of Membrane Science, 303 (2007) 221-233.
600 [29] M. Takeuchi , K. Sakamoto ,G.Martra. et ac., Mechanism of Photoinduced Superhydrophilicity on
601 the TiO2 Photocatalyst Surface, J. Phys. Chem. B, 109 (2005)15422–15428
602 [30] A.R. Khataee, V. Vatanpour, A.R. Amani Ghadim, Decolorization of C.I. Acid Blue 9 solution by
603 UV/Nano-$TiO_2$, Fenton, Fenton-like, electro-Fenton and electrocoagulation processes: A comparative
604 study, J Hazard Mater, 161 (2009) 1225-1233.